Biochemical and Biophysical Research Communications 421 (2012) 544–549

Contents lists available at SciVerse ScienceDirect

Biochemical and Biophysical Research Communications

journal homepage: www.elsevier.com/locate/ybbrc

The functional analysis of the CHMP2B missense mutation associated with neurodegenerative diseases in the endo-lysosomal pathway

Jeong-Ho Han [a,1], Hyun-Hee Ryu [a,1], Mi-Hee Jun [a], Deok-Jin Jang [b], Jin-A. Lee [a,*]

[a] Department of Biotechnology, College of Life Science and Nano Technology, Hannam University, 461-6, Jeonmin-dong, Yuseong-gu, Daejeon 305-811, Republic of Korea
[b] Department of Applied Biology, College of Ecology and Environment, Kyungpook National University, 386, Gajang-dong, Sangju-si, Kyeongbuk 742-711, Republic of Korea

ARTICLE INFO

Article history:
Received 3 April 2012
Available online 13 April 2012

Keywords:
CHMP2B
Endocytosis
Autophagy
ESCRT
Neurodegenerative disease

ABSTRACT

Endosomal sorting complexes required for transport (ESCRTs) regulate a key sorting step of protein trafficking between endosomal compartments in lysosomal degradation. Interestingly, mutations in charged multivesicular body protein 2B (CHMP2B), which is a core subunit of ESCRT-III, have been identified in some neurodegenerative diseases. However, the cellular pathogenesis resulting from CHMP2B missense mutations is unclear. Furthermore, little is known about their functional analysis in post-mitotic neurons. In order to examine their cellular pathogenesis, we analyzed their effects in the endo-lysosomal pathway in post-mitotic neurons. Interestingly, of the missense mutant proteins, $CHMP2B^{T104N}$ mostly accumulated in the Rab5- and Rab7-positive endosomes and caused delayed degradation of EGFR as compared to $CHMP2B^{WT}$. Furthermore, $CHMP2B^{T104N}$ showed less association with Vps4 ATPase and was avidly associated with Snf7-2, a core component of ESCRT-III, suggesting that it may cause defects in the process of dissociation from ESCRT. Of the missense variants, $CHMP2B^{T104N}$ caused prominent accumulation of autophagosomes. However, neuronal cell survival was not dramatically affected by expression of $CHMP2B^{T104N}$. These findings suggested that, from among the various missense mutants, $CHMP2B^{T104N}$ was associated with relatively mild cellular pathogenesis in post-mitotic neurons. This study provided a better understanding of the cellular pathogenesis of neurodegenerative diseases associated with various missense mutations of CHMP2B as well as endocytic defects.

1. Introduction

Endosomal sorting complexes required for transport (ESCRTs) are involved in cargo protein trafficking from endosomes to lysosomes. ESCRTs are composed of four different heteromeric protein complexes, ESCRT-0, -I, -II and III, which are sequentially and transiently recruited from the cytosol to endosomal membranes [1,2]. ESCRTs recognize ubiquitinated cargo proteins and sort them into endosomal membranes leading to invagination of the cargo proteins into the intraluminal vesicles [3–5]. The ESCRT complexes dissociate from the endosomes by the action of Vps4 ATPase via ATP hydrolysis and are thus recycled for the next round of assembly of ESCRT [6,7].

A growing body of evidence has suggested that ESCRTs are involved in various biological processes including cytokinesis, viral budding, autophagy, transcriptional regulation, endosomal sorting and trafficking [2,8]. ESCRT dysfunction is associated with human diseases such as cancer, myopathy and neurodegeneration [9–11]. Dysregulation of the components, such as mahogunin or CHMP1B, which are associated with the ESCRT pathway can cause spongiform neurodegeneration [12–14]. Moreover, mutations in CHMP2B, which is a key component of ESCRT-III, have been reported in Frontotemporal dementia (FTD), FTD with motor neuron disease (FTD–MND) and Amyotrophic lateral sclerosis (ALS) [15]. The first observed mutation in CHMP2B was identified in chromosome 3 (FTD-3) and linked to cases of autosomal dominant presenile dementia [16]. The point mutation in the 5′ acceptor splice site of exon 6 produces two abnormal transcripts resulting in the generation of $CHMP2B^{Intron5}$ which results in C-terminal truncation of 36 amino acids and $CHMP2B\Delta^{10}$, replacing these with 29 amino acids which are different than the wild-type. Intriguingly, expression of the $CHMP2B^{Intron5}$ in various mammalian cells and cortical neurons resulted in endocytic and autophagic defects [17,18]. Moreover, $CHMP2B^{Intron5}$ transgenic mice have been reported to show progressive neuronal inclusion formation and axonal degeneration [19]. Other C-terminal truncation mutations such as Q165X or R186X were identified in a Belgian family with FTLD and an Afrikaner family with FTD, respectively. The Q165X mutation has been known to cause cellular toxicity in a mammalian cell culture model [20–22].

Several missense mutations of CHMP2B have also been reported in some neurodegenerative diseases including FTD [15]. The D148Y

* Corresponding author. Fax: +82 42 629 8769.
E-mail address: leeja@hnu.kr (J.-A. Lee).
[1] These authors are equally contributed to this work.

0006-291X/$ - see front matter © 2012 Elsevier Inc. All rights reserved.
http://dx.doi.org/10.1016/j.bbrc.2012.04.041

mutation identified in a case of FTD-3 in a Danish family was found not to be pathogenic in cultured neurons [16,17]. Since then, other missense mutations (Q206H, I29V and T104N) have been identified in familial or sporadic cases of ALS [23,24]. Moreover, other N143S and S194L CHMP2B missense variants have been reported in familial patients with cortical basal degeneration (CBD) or pro-band with familial frontotemporal lobar degeneration (FTLD), respectively [21,25]. Even though there are a few reported studies about the effects of CHMP2B missense variants in mammalian cell lines, or revealing expectations regarding their pathogenic characteristics, little is known about their pathogenic nature in post-mitotic neurons [15,23–25].

In this study, we investigated the effect of CHMP2B missense variants (Q206H, I29V, T104N, N143S and S194L) in the endo-lysosomal pathway of post-mitotic neurons. Intriguingly, of these missense variants, CHMP2B^{T104N} accumulated prominently in rab5- and rab7-positive endosomes and delayed EGFR degradation. Moreover, CHMP2B^{T104N}, as compared to CHMP2B^{WT}, was less associated with VPS4 ATPase and likely results in its abnormal association with Snf7-2. In addition, CHMP2B^{T104N} expression caused autophagosome accumulation. Despite these cellular defects in the endosomal pathway, neuronal cell survival was not dramatically affected by its expression in our cultured neurons. This was the first study to demonstrate the effects of various missense mutations in post-mitotic neurons. Our results suggested that, from among the assessed missense mutations, CHMP2B^{T104N} is potentially associated with endosomal impairments, a result likely due to defects in the dissociation of ESCRTs in post-mitotic neurons.

2. Materials and methods

2.1. Molecular cloning

Each CHMP2B mutation was generated by recombinant PCR using specific primers containing each missense mutation (Supplementary Table 1) [17]. For mammalian expression, each CHMP2B DNA fragment was subcloned into a 3Xflag CMV7.1 vector (Sigma) and into the BglII-XbaI site (Supplementary Table 1).

2.2. Cell cultures, transfection and immunocytochemistry

Cortical neurons from E17-18 Sprague-Dawley rats (Samtako Co., Korea) were cultured as reported previously [17,26]. Each DNA construct was transfected with Lipofectamine (Invitrogen) according to the manufacturer's protocol into cortical neurons at 5–7 DIV. For immunostaining, 24 h after transfection the cortical neurons were fixed with 4% paraformaldehyde for 10 min, permeabilized with 0.1% Triton X 100 for 5 min and then blocked with 3% bovine serum albumin (BSA) for 1 h at room temperature. The cortical neurons were incubated anti-flag M2 antibody (Sigma, 1:100) or anti-cmyc antibody (Thermo Sci., 1:200) for 1 h and then in anti-cy3 or anti-DyLight 488 Secondary antibody for 1 h at room temperature. The neurons were examined using a LSM 510 Confocal Laser Scanning Microscope (Carl Zeiss). For the cell survival assay, 2–3 days after transfection, the cell viability was assessed using a propidium iodide (PI) exclusion assay (Roche). The GFP positive and PI negative cells were counted as neurons which survived.

2.3. Co-immunoprecipitation and western blotting

Twenty-four hours after transfection, the HEK 293 cells were homogenized in immunoprecipitation (IP) lysis buffer (50 mM of Tris–HCl at pH 7.5, 150 mM of NaCl, 1% NP40, 0.5% sodium deoxycholate and protease inhibitor). The total cell lysates were incubated with 3 μg of anti-flag antibody overnight at 4 °C and then incubated with protein G-agarose for 7 h. The immunoprecipitated complexes were washed with IP washing buffer (50 mM of Tris–HCl at pH 7.5, 150 mM of NaCl, 1% NP40, 0.5% sodium deoxycholate and protease inhibitor). The samples were analyzed by Western blotting with anti-flag antibody (1:20000) or anti-cmyc antibody (1:2000), and HRP-conjugated anti-mouse secondary antibody (1:20000).

2.4. Protein and EGFR degradation assays

For the EGFR degradation assay, 24 h after transfection the cells were starved in FBS-free DMEM (Thermo Scientific) for 3 h. Human EGF (100 ng/ml), together with cycloheximide (30 μg/ml) for inhibition of new protein synthesis, was incubated for the indicated time (30, 60, 120, 240 min). The EGFR degradation was examined by Western blot analysis using anti-EGFR (1:500, Santa Cruz Biotechnology) and HRP-conjugated anti-rabbit secondary antibodies (1:10000).

3. Results and discussions

3.1. The generation of missense variants of CHMP2B

To date, several missense variants of CHMP2B have been identified in FTD cases including FTD–MND and CBD [15]. However, little is known about their effects on the endo-lysosomal and autophagy pathways, and cell survival in post-mitotic neurons.

In this study, in order to investigate the effects of missense mutations of CHMP2B, 5 missense variants (p.Q206H, p.I29V, p.T104N, p.N143S and p.S194L) were chosen whose pathogenic nature in post-mitotic neurons have remained undetermined [15]. As shown in Fig. 1, except for the Q206H or S194L missense variants, most CHMP2B missense mutations occur in the conserved Snf7 domain. In order to verify whether or not there were any differences between the CHMP2B wild-type (WT) and CHMP2B missense variants in terms of their expression levels 24 h after transfection in HEK 293 cells, Western blot analysis was performed using anti-flag antibody. As shown in Fig. 1B, their expression levels were nearly the same. Therefore, the effects of the missense variants in the endo-lysosomal pathway would not be due to differences in their expression levels. Although *in silico* analysis of the identified amino acid substitutions predicted that p.S194L, p.I29V and p.Q206H missense mutations would decrease protein stability [24], we checked that their protein stability was not decreased, indicating that protein stability may not be a pathogenic factor (data not shown).

3.2. The subcellular localization of missense variants of CHMP2B in post-mitotic neurons

In order to compare the localization of CHMP2B missense variants in post-mitotic neurons, cultured cortical neurons at DIV5-7 (*in vitro,* day 5–7) were transfected with each variant construct. As shown in Fig. 2, most CHMP2B mutant proteins similar to CHMP2B^{WT} were localized in the cytoplasm. They showed a diffused expression pattern because the ESCRT-III components were transiently recruited into endosomes. However, of the missense mutant proteins, CHMP2B^{T104N}, CHMP2B^{N143S} and CHMP2B^{Q206H} appeared in a dot-like expression pattern within the cytoplasm (Fig. 2).

In order to further examine their localization within the cytoplasm, either rab5-GFP (an early endosome marker) or rab7-GFP (a late endosome marker) was cotransfected with each mutant

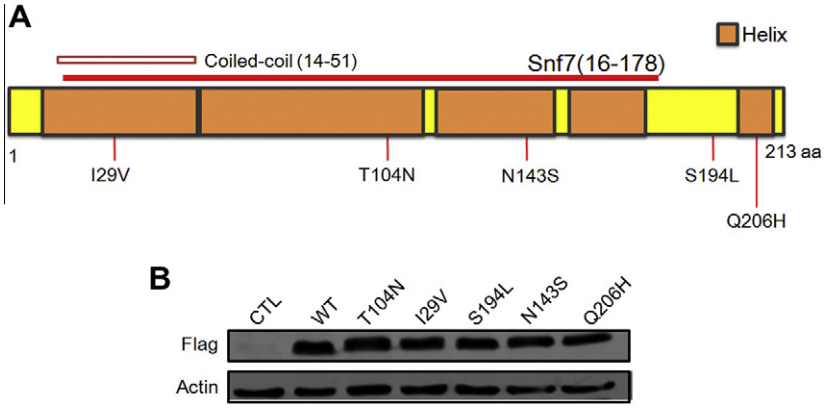

Fig. 1. CHMP2B missense mutations and their protein expression in HEK 293 cells. (A) CHMP2B missense mutations in FTD and MND. CHMP2B has five helix structures, a conserved Snf7 domain and a coiled coil domain. (B) Protein expression for each HEK 293 cell missense variant. Flag-CHMP2B^{WT} or each Flag-missense CHMP2B was transfected into HEK 293 cells. Twenty four hours after transfection a Western blot was performed using anti-Flag antibody.

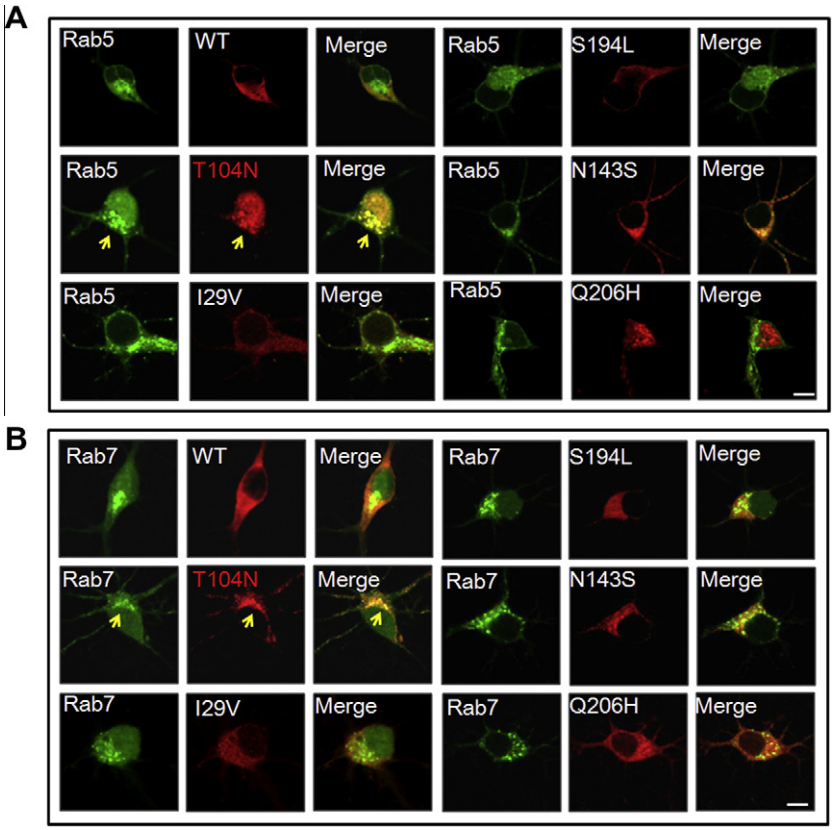

Fig. 2. Cellular localization of each CHMP2B missense variant in post-mitotic neurons. Cellular localization for each CHMP2B mutant in rab5-GFP (A) or rab7-GFP expressed neurons (B). Rab5-GFP or rab7-GFP, together with each flag-tagged missense variant of CHMP2B, was transfected into cultured cortical neurons at 5 DIV. Twenty four hours after transfection, immunostaining was carried out using anti-flag antibody and anti-mouse cy3-conjugated secondary antibody. Arrows indicate the accumulation of CHMP2B^{T104N} in the endosomes. Scale bar, 10 μm.

construct. As shown in Fig. 2, only CHMP2B^{T104N} was co-localized with rab5- and rab7-positive endosomes, not CHMP2B^{N143S} or CHMP2B^{Q206H}, indicating defects in the trafficking between the endosomes and the cytosol. A previous study demonstrated that CHMP2B^{I29V} and CHMP2B^{Q206H} missense mutants caused cytoplasmic vacuoles in HEK 293 cells [24], yet we found that the other missense mutant proteins did not accumulate in the endosomes of our neuronal cell model. Even though we could not exclude the possibility that another missense mutant could cause cellular defects with a longer incubation period or in a different assay system, in this study we decided to focus on the functional analysis of CHMP2B^{T104N}.

3.3. *CHMP2B^{T104N} delayed the degradation of EGFR*

If CHMP2B^{T104N} accumulated in the endosomes, the trafficking and degradation of cargo proteins may be affected in CHMP2B^{T104N} expressed cells. In order to determine the effect of CHMP2B^{T104N} on the degradation of cargo proteins, the degradation of EGFR which is a well known receptor degraded via endo-lysosomal pathway was

examined [27]. The CHMP2B^{WT} or CHMP2B^{T104N} expressed cells were treated with human EGF (100 ng/ml) to activate EGFR in the endosomal pathway. As shown in Fig. 3A and B 60 min after application of EGF the expressed EGFR remained more intact in the cells expressing CHMP2B^{T104N} than in the cells expressing CHMP2B^{WT}, suggesting that EGFR degradation was delayed in the cells expressing CHMP2B^{T104N}. However, we did not see differences in EGFR degradation between CHMP2B^{WT} and the other missense variants (CHMP2B^{N143S} or CHMP2B^{Q206H}), which slightly accumulated in the cytoplasm as shown in Fig. 2 (Supplementary Fig. 1). Thus, missense mutation in p.N143S and p.Q206H were unlikely to be associated with endocytic defects. Taken together, these results suggested that accumulation of CHMP2B^{T104N} in the endosome is associated with defects in the degradation process of cargo proteins in the endosomal pathway.

3.4. As compared to CHMP2B^{WT}, CHMP2B^{T104N} is less associated with VPS4B

How does CHMP2B^{T104N} accumulate in endosomes and delay EGFR degradation?

An ESCRT-III such as CHMP2B is thought to be dissociated from the endosomal membrane via VPS4, a dissociator of ESCRT components. Interestingly, although its severity of action may be different, the cellular phenotype of CHMP2B^{T104N} is very similar with that of the C-terminal truncation mutant (data not shown) [17,21]. The C-terminal of CHMP2B is known to be an autoinhibitory domain functioning to prevent self-interaction or abnormal interaction with other components during endosomal trafficking. Moreover, the C-terminal MIT domain interacting motif (MIM) can recruit VPS4 [28]. Therefore, we investigated whether or not CHMP2B^{T104N} demonstrates defects in the ability to recruit VPS4. For this effort we examined the interaction between CHMP2B^{T104N} and VPS4B using co-immunoprecipitation, and then compared their interactions with those of VPS4 and CHMP2B^{WT} or CHMP2B^{Intron5}. For this, Flag-CHMP2B and VPS4B-cmyc were transfected into HEK 293 cells and 24 h later the cell lysates were used for an immunoprecipitation experiment. As expected, the interaction of CHMP2B^{Intron5} with VPS4B was greatly reduced because the C-terminal region is required for its interaction with VPS4 (Fig. 3C and D). Intriguingly, CHMP2B^{T104N} was significantly less associated with VPS4B as compared to CHMP2B^{WT}, yet more associated with VPS4B as compared to CHMP2B^{Intron5} (Fig. 3C and D). In addition, CHMP2B is known to associate with Vps20-Snf7-Vps24 in order to complete the ESCRT-III assembly [2]. Using co-immunoprecipitation, we investigated if the CHMP2B^{T104N} mutation affects its association with Snf7-2, a major component of ESCRT-III. As shown Fig. 3C and D, the CHMP2B^{Intron5} is more avidly associated with Snf7-2 as compared to CHMP2B^{WT}, a result which agrees with a previous report [17]. The interaction of CHMP2B^{T104N} with Snf7-2 also increased as compared to that of CHMP2B^{WT}. The interaction between CHMP2B^{T104N} and Snf7-2 was reduced as compared to that of CHMP2B^{Intron5} and Snf7-2 (Fig. 3E and F). This result can be explained by the dissociation defects of ESCRT-III which occur via impairment of VPS4 recruitment. Taken together, this data indicated that the CHMP2B^{T104N} mutant can affect interaction with VPS4 ATPase and may cause impairment of the dissociation of ESCRTs, such as CHMP2B and Snf7, from endosomes.

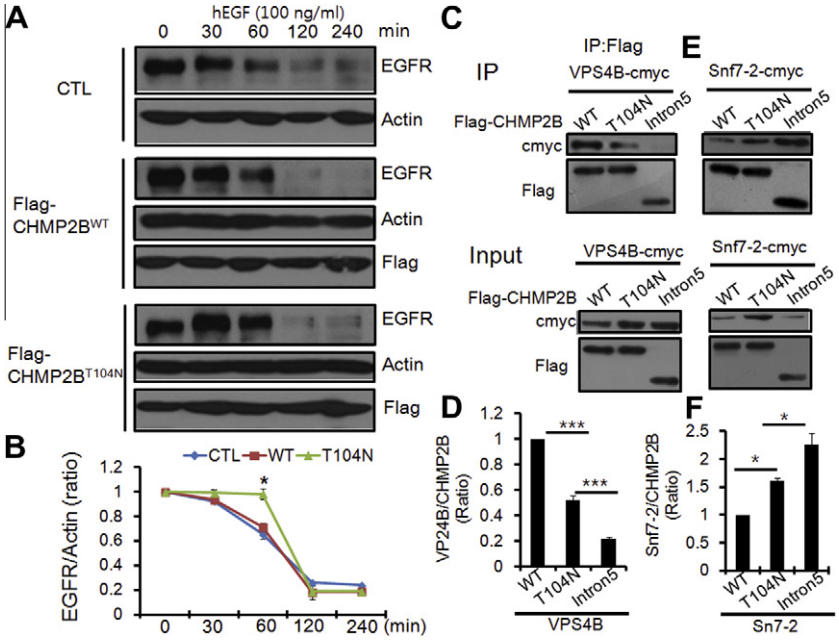

Fig. 3. CHMP2B^{T104N} delayed EGFR degradation and caused abnormal association with VPS4B or Snf7-2. (A) EGFR degradation assay in GFP, CHMP2B^{WT} or CHMP2B^{T104N} as expressed in HEK 293 cells. GFP, Flag-CHMP2B^{WT} or Flag-CHMP2B^{T104N} was transfected into HEK 293 cells. Twenty four hours after transfection, the cells were incubated in serum free DMEM for 3 h and then treated with human EGF (100 ng/ml) together with cycloheximide (CHX) (30 μg/ml) during the indicated time (0, 30, 60, 120, 240 min). Western blot was performed in cell lysates using either anti-EGFR or anti-actin antibody, and HRP-conjugated anti-rabbit or anti-mouse secondary antibody, respectively. (B) The graph shows quantification of the EGFR protein level during each indicated time after EGF treatment. The level of EGFR was normalized to that of the actin used as a loading control. Normalized relative EGFR level (EGFR/actin) was considered to be 1 at 0 min after EGF treatment. Each measured EGFR level at each indicated time was normalized by the EGFR level at 0 min. $^{*}p < 0.05$ (one way ANOVA-test, Tukey's multiple comparison test). (C and E) The association of CHMP2B^{T104N} with either VPS4B or Snf7-2. Flag-CHMP2B (WT, T104N or Intron5) together with VPS4B-cmyc were cotransfected into HEK 293 cells. Twenty four hours after transfection, immunoprecipitation using anti-flag antibody was performed on the cell lysates. Subsequent Western blot analysis was performed using anti-cmyc and anti-flag antibodies. (D and F) The bar graphs represent the relative ratios of the associations between CHMP2B (WT, T104N or Intron5) and either VPS4B or Snf7-2. The association level of the immunoprecipitates (VPS4B-cmyc or Snf7-2-cmyc) was determined by normalization using flag-CHMP2B (WT, T104N or Intron5). The association between CHMP2B^{WT} and either VPS4B or Snf7-2 was considered to be 1. $^{*}p < 0.05$; $^{***}p < 0.001$ (one way ANOVA-test, Tukey's multiple comparison test). Values represent mean ± SEM of three independent cultures and experiments for each condition.

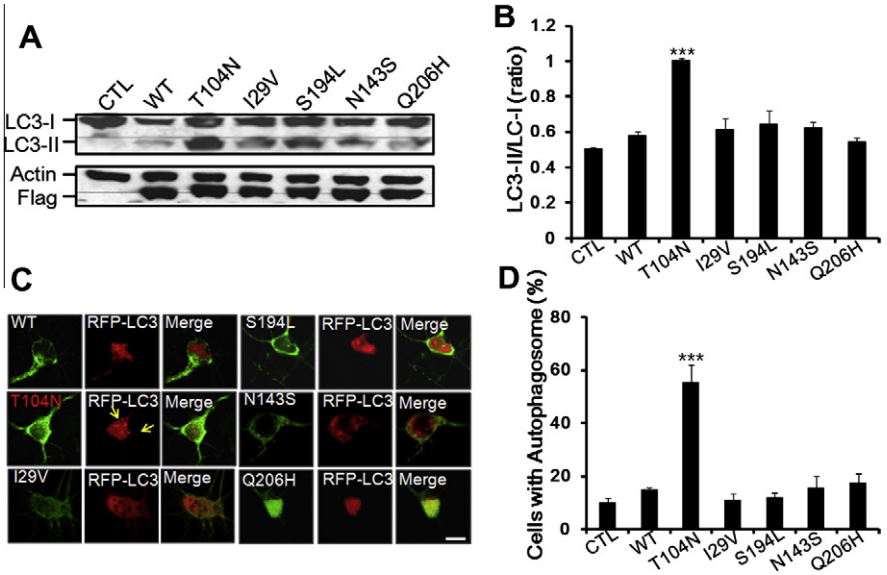

Fig. 4. CHMP2B^{T104N} caused accumulation of autophagosomes but didn't affect neuronal cell survival. (A) GFP (as a control) or each Flag-CHMP2B variant was transfected into HEK293 cells, and 24 h after transfection a Western blot analysis was carried out using anti-LC3 antibody. (B) The bar graph represents the level of LC3-II/LC3-I in the control or cells expressing CHMP2B. $^{***}p < 0.001$ (one way ANOVA-test, Tukey's multiple comparison test). (C) RFP-LC3, together with each flag-CHMP2B, was transfected into cultured cortical neurons. Twenty four hours after transfection, immunostaining was performed using anti-flag antibody and FITC-conjugated anti-mouse secondary antibody. Arrows indicate RFP-LC3 positive autophagosomes. Scale bar, 20 μm. (D) The graph indicates the percentage of cells with autophagosomes. $^{***}p < 0.001$ (one way ANOVA-test, Tukey's multiple comparison test). Values represent mean ± SEM of three independent cultures and experiments for each condition.

3.5. CHMP2B^{T104N} caused accumulation of autophagosomes but did not affect neuronal cell survival

Previous work reported that a C-terminal truncation mutant of CHMP2B caused the accumulation of autophagosomes resulting in the impairment of the fusion step between autophagosome and lysosome [17,18]. In order to further determine whether or not missense mutations also affect the autophagy pathway, LC3-II level was examined using Western blot analysis. Interestingly, LC3-II was observed to be strongly increased in CHMP2B^{T104N} expressed cells as compared to the other mutant proteins or CHMP2B^{WT} expressed neurons (Fig. 4A and B). Furthermore, RFP-LC3 positive autophagosomes accumulated prominently in CHMP2B^{T104N} expressed neurons but not in other mutants or CHMP2B^{WT} expressed neurons. This data was consistent with recent findings that suggest that ESCRT dysfunction can result in autophagosome accumulation [9,29].

If CHMP2B^{T104N} affects endocytic trafficking and degradation, and the autophagy pathway, what about its effect on neuronal cell survival? A previous study using a mammalian neuron culture system and recent work using CHMP2B^{Intron5} transgenic mice have demonstrated that the presence of the CHMP2B^{Intron5} mutation reduced neuronal cell survival, suggesting it is toxic. In order to examine if CHMP2B^{T104N} affects neuronal cell survival, the CHMP2B^{T104N} mutant construct was transfected into mature cortical neurons and the surviving neurons were counted 2–3 days after transfection as previously reported [17]. As shown in Supplementary Fig. 2, neurons expressing CHMP2B^{Intron5} showed reduced cell survival 2–3 days after transfection. However, neurons expressing CHMP2B^{T104N} did not show a difference in cell survival as compared to the neurons expressing CHMP2B^{WT}. We examined neuronal cell survival 5–6 days after transfection but didn't see a considerable change in the neuronal cell death rate in the neurons expressing CHMP2B^{T104N} (data not shown). Although we cannot exclude the possibility that CHMP2B^{T104N} could cause neuronal cell death when evaluated over a period longer than a few days, CHMP2B^{T104N} did not cause the severe rapid cell death as seen with CHMP2B^{Intron5}, suggesting that this mutation causes mild cellular pathogenesis associated with endo-lysosomal defects when compared to C-terminal truncation mutations.

In summary, of the five missense variants, CHMP2B^{T104N} caused its abnormal accumulation in endosomes, probably via a mechanism of lower association with VPS4B, which is involved in dissociation of ESCRT-III components, and delayed EGFR degradation. Moreover, autophagosomes accumulated considerably in the neurons expressing CHMP2B^{T104N}. However, CHMP2B^{T104N} did not cause rapid neuronal cell death. Therefore, we propose that the T104N mutant causes neurodegeneration associated with mild endo-lysosomal impairment as enabled by several disease-causing mechanisms. Accumulation of these cellular defects may lead to age-dependent neurodegenerative diseases such as FTD or ALS. Further work and clarification are needed in order to fully elucidate the role and importance of the CHMP2B missense mutation in FTD or MND, *in vivo*, using a missense mutant transgenic mouse model. Further detailed biochemical studies or structural studies are also required regarding how the substitution of threonine by asparagine affects the function and structure of CHMP2B. One of the possibilities for mechanism is the change in phosphorylation state as the naïve threonine site associated with the p.T104N change is predicted to be a site of phosphorylation [24]. Thus, it will be interesting to determine if this change affects protein structures or protein interactions.

Our findings provide a better understanding of the cellular pathogenesis of neurodegenerative diseases associated with CHMP2B missense mutations, as well as several relevant neurodegenerative disorders.

Acknowledgments

This work was supported by a grant from the Korean Health Technology R&D Project, Ministry for Health, Welfare, & Family Affairs, Republic of Korea (A100488) and by the Basic Science Research Program through the NRF funded by the Ministry of Education, Science, and Technology (2010-0010824).

Appendix A. Supplementary data

Supplementary data associated with this article can be found, in the online version, at http://dx.doi.org/10.1016/j.bbrc.2012.04.041.

References

[1] J.H. Hurley, E. Boura, L.A. Carlson, B. Rozycki, Membrane budding, Cell 143 (2010) 875–887.
[2] O. Schmidt, D. Teis, The ESCRT machinery, Curr. Biol. 22 (2012) R116–R120.
[3] M. Babst, D.J. Katzmann, E.J. Estepa-Sabal, T. Meerloo, S.D. Emr, Escrt-III: an endosome-associated heterooligomeric protein complex required for mvb sorting, Dev. Cell 3 (2002) 271–282.
[4] M. Babst, D.J. Katzmann, W.B. Snyder, B. Wendland, S.D. Emr, Endosome-associated complex, ESCRT-II, recruits transport machinery for protein sorting at the multivesicular body, Dev. Cell 3 (2002) 283–289.
[5] D.J. Katzmann, M. Babst, S.D. Emr, Ubiquitin-dependent sorting into the multivesicular body pathway requires the function of a conserved endosomal protein sorting complex, ESCRT-I, Cell 106 (2001) 145–155.
[6] B.A. Davies, I.F. Azmi, J. Payne, A. Shestakova, B.F. Horazdovsky, M. Babst, D.J. Katzmann, Coordination of substrate binding and ATP hydrolysis in Vps4-mediated ESCRT-III disassembly, Mol. Biol. Cell 21 (2010) 3396–3408.
[7] M.A. Adell, D. Teis, Assembly and disassembly of the ESCRT-III membrane scission complex, FEBS Lett. 585 (2011) 3191–3196.
[8] I. Roxrud, H. Stenmark, L. Malerod, ESCRT & Co, Biol. Cell 102 (2010) 293–318.
[9] T.E. Rusten, A. Simonsen, ESCRT functions in autophagy and associated disease, Cell Cycle 7 (2008) 1166–1172.
[10] S. Saksena, S.D. Emr, ESCRTs and human disease, Biochem. Soc. Trans. 37 (2009) 167–172.
[11] S. Stuffers, A. Brech, H. Stenmark, ESCRT proteins in physiology and disease, Exp. Cell Res. 315 (2009) 1619–1626.
[12] B.Y. Kim, J.A. Olzmann, G.S. Barsh, L.S. Chin, L. Li, Spongiform neurodegeneration-associated E3 ligase Mahogunin ubiquitylates TSG101 and regulates endosomal trafficking, Mol. Biol. Cell 18 (2007) 1129–1142.
[13] J. Jiao, K. Sun, W.P. Walker, P. Bagher, C.D. Cota, T.M. Gunn, Abnormal regulation of TSG101 in mice with spongiform neurodegeneration, Biochim. Biophys. Acta 1792 (2009) 1027–1035.
[14] E. Reid, J. Connell, T.L. Edwards, S. Duley, S.E. Brown, C.M. Sanderson, The hereditary spastic paraplegia protein spastin interacts with the ESCRT-III complex-associated endosomal protein CHMP1B, Hum. Mol. Genet. 14 (2005) 19–38.
[15] A.M. Isaacs, P. Johannsen, I. Holm, J.E. Nielsen, Frontotemporal dementia caused by CHMP2B mutations, Curr. Alzheimer Res. 8 (2011) 246–251.
[16] G. Skibinski, N.J. Parkinson, J.M. Brown, L. Chakrabarti, S.L. Lloyd, H. Hummerich, J.E. Nielsen, J.R. Hodges, M.G. Spillantini, T. Thusgaard, S. Brandner, A. Brun, M.N. Rossor, A. Gade, P. Johannsen, S.A. Sorensen, S. Gydesen, E.M. Fisher, J. Collinge, Mutations in the endosomal ESCRTIII-complex subunit CHMP2B in frontotemporal dementia, Nat. Genet. 37 (2005) 806–808.
[17] J.A. Lee, A. Beigneux, S.T. Ahmad, S.G. Young, F.B. Gao, ESCRT-III dysfunction causes autophagosome accumulation and neurodegeneration, Curr. Biol. 17 (2007) 1561–1567.
[18] M. Filimonenko, S. Stuffers, C. Raiborg, A. Yamamoto, L. Malerod, E.M. Fisher, A. Isaacs, A. Brech, H. Stenmark, A. Simonsen, Functional multivesicular bodies are required for autophagic clearance of protein aggregates associated with neurodegenerative disease, J. Cell Biol. 179 (2007) 485–500.
[19] S. Ghazi-Noori, K.E. Froud, S. Mizielinska, C. Powell, M. Smidak, M. Fernandez de Marco, C. O'Malley, M. Farmer, N. Parkinson, E.M. Fisher, E.A. Asante, S. Brandner, J. Collinge, A.M. Isaacs, Progressive neuronal inclusion formation and axonal degeneration in CHMP2B mutant transgenic mice, Brain 135 (2012) 819–832.
[20] P. Momeni, E. Rogaeva, V. Van Deerlin, W. Yuan, J. Grafman, M. Tierney, E. Huey, J. Bell, C.M. Morris, R.N. Kalaria, S.J. van Rensburg, D. Niehaus, F. Potocnik, T. Kawarai, S. Salehi-Rad, C. Sato, P. St George-Hyslop, J. Hardy, Genetic variability in CHMP2B and frontotemporal dementia, Neurodegener. Dis. 3 (2006) 129–133.
[21] J. van der Zee, H. Urwin, S. Engelborghs, M. Bruyland, R. Vandenberghe, B. Dermaut, T. De Pooter, K. Peeters, P. Santens, P.P. De Deyn, E.M. Fisher, J. Collinge, A.M. Isaacs, C. Van Broeckhoven, CHMP2B C-truncating mutations in frontotemporal lobar degeneration are associated with an aberrant endosomal phenotype in vitro, Hum. Mol. Genet. 17 (2008) 313–322.
[22] H. Urwin, A. Authier, J.E. Nielsen, D. Metcalf, C. Powell, K. Froud, D.S. Malcolm, I. Holm, P. Johannsen, J. Brown, E.M. Fisher, J. van der Zee, M. Bruyland, C. Van Broeckhoven, J. Collinge, S. Brandner, C. Futter, A.M. Isaacs, Disruption of endocytic trafficking in frontotemporal dementia with CHMP2B mutations, Hum. Mol. Genet. 19 (2010) 2228–2238.
[23] N. Parkinson, P.G. Ince, M.O. Smith, R. Highley, G. Skibinski, P.M. Andersen, K.E. Morrison, H.S. Pall, O. Hardiman, J. Collinge, P.J. Shaw, E.M. Fisher, ALS phenotypes with mutations in CHMP2B (charged multivesicular body protein 2B), Neurology 67 (2006) 1074–1077.
[24] L.E. Cox, L. Ferraiuolo, E.F. Goodall, P.R. Heath, A. Higginbottom, H. Mortiboys, H.C. Hollinger, J.A. Hartley, A. Brockington, C.E. Burness, K.E. Morrison, S.B. Wharton, A.J. Grierson, P.G. Ince, J. Kirby, P.J. Shaw, Mutations in CHMP2B in lower motor neuron predominant amyotrophic lateral sclerosis (ALS), PLoS One 5 (2010) e9872.
[25] M. Ghanim, L. Guillot-Noel, F. Pasquier, L. Jornea, V. Deramecourt, B. Dubois, I. Le Ber, A. Brice, CHMP2B mutations are rare in French families with frontotemporal lobar degeneration, J. Neurol. 257 (2010) 2032–2036.
[26] J.A. Lee, F.B. Gao, Inhibition of autophagy induction delays neuronal cell loss caused by dysfunctional ESCRT-III in frontotemporal dementia, J. Neurosci. 29 (2009) 8506–8511.
[27] C.E. Futter, A. Pearse, L.J. Hewlett, C.R. Hopkins, Multivesicular endosomes containing internalized EGF-EGF receptor complexes mature and then fuse directly with lysosomes, J. Cell Biol. 132 (1996) 1011–1023.
[28] M.D. Stuchell-Brereton, J.J. Skalicky, C. Kieffer, M.A. Karren, S. Ghaffarian, W.I. Sundquist, ESCRT-III recognition by VPS4 ATPases, Nature 449 (2007) 740–744.
[29] D. Metcalf, A.M. Isaacs, The role of ESCRT proteins in fusion events involving lysosomes, endosomes and autophagosomes, Biochem. Soc. Trans. 38 (2010) 1469–1473.